11. Neary D, Snowden JS, Northen B, Goulding P. Dementia of the frontal lobe type. *J Neurol Neurosurg Psych* 1988;51:353–361.
12. Ohnishi T, Hoshi H, Jinnouchi S, Nagamachi S, Wantanabe K, Mituyama Y. The utility of cerebral blood flow imaging in patients with unique syndrome of progressive dementia with motor neuron disease. *J Nucl Med* 1990;31:688–691.
13. Risberg J, Passant U, Warkentin S, Gustafson L. Regional blood flow in frontal lobe dementia of non-Alzheimer type. *Dementia* 1993;4:186–187.
14. Van Heertum RL. Clinical diagnosis: major depressive disorder. In: Van Heertum RL, Tikofsky RS, eds. *Cerebral SPECT imaging*, 2nd ed. New York: Raven Press; 1995:194.
15. Pohl P, Vogel G, Fill H, Rössler H, Zangerle R, Gerstenbrand F. Single-photon emission computed tomography in AIDS dementia complex. *J Nucl Med* 1988;29: 1382–1386.
16. Costa DC, Ell P, Burns A, Philpot M, Levy R. CBF tomograms with ^{99m}Tc-HMPAO in patients with dementia (Alzheimer type and HIV) and Parkinson's disease–initial results. *J Cereb Blood Flow Metab* 1988;8:S109–S115.
17. Neary D, Snowden JS, Mann DMA. The clinical pathological correlates of lobar atrophy. *Dementia* 1993;4:143–149.
18. Moretti JL, Sergent A, Louarn F et. al. Cortical perfusion assessment with ^{123}I-isopropyl amphetamine (^{123}I-AMP) in normal pressure hydrocephalus (NPH). *Eur J Nucl Med* 1988;14:73–79.
19. Cole MG, Dastoor D. A new hierarchic approach to the measurement of dementia. *Psychosomatics* 1987;28:298–305.
20. McKhann G, Drachman D, Folstein M, Katzman R, Price D, Stadlan EM. Clinical diagnosis of Alzheimer's disease: report of the NINCDS-ADRDA Work Group under the auspices of Department of Health and Human Services Task Force on Alzheimer's disease. *Neurol* 1984;34:939–944.
21. Holman BL, Johnson KA, Greada B, Carvalho PA, Smith A. The Scintigraphic appearance of Alzheimer's disease: a prospective study using technetium-99m-HMPAO SPECT. *J Nucl Med* 1992;33:1941–185.
22. Johnson KA, Holman BL, Mueller SP, et al. Single-photon emission computed tomography in Alzheimer's disease. Abnormal I-123-iofetamine uptake reflects dementia severity. *Arch Neurol* 1988:45–392-396.
23. Eagger S, Syed GMS, Burns A, Barette JJ, Levy R. Morphologic (CT), and functional (rCBF SPECT) correlates in Alzheimer's disease. *Nucl Med Commun* 1992;13:644–647.
24. Wolfe N, Reed BR, Eberling JL, Jagust WJ. Temporal lobe perfusion on single-photon emission computed tomography predicts the rate of cognitive decline in Alzheimer's disease. *Arch Neurol* 1995;52:257–262.
25. Perani D, DiPiero V, Vallar G, et al. Technetium-99m-HMPAO-SPECT study of regional cerebral perfusion in early Alzheimer's disease. *J Nucl Med* 1988;29:1507–1514.
26. McGeer PL, Kamo H, Harrop R, et. al Comparison of PET, MRI, and CT with pathology in a proven case of Alzheimer's disease. *Neurol* 1986;36:1569–1574.
27. Jobst KA, Smith AD, Barker CS, et al. Association of atrophy of the medial temporal lobe with reduced blood flow in the posterior parietotemporal cortex in patients with a clinical and pathological diagnosis of Alzheimer's disease. *J Neurol Neurosurg Psych* 1992;55:190–194.
28. Launes J, Sulkava R, Erkinjuntti T, et al. Technetium-99m-HMPAO SPECT in suspected dementia. *Nucl Med Commun* 1991;12:757–765.

Imaging Beta-Adrenoceptors in the Human Brain with (*S*)-1′-[^{18}F]Fluorocarazolol

Aren van Waarde, Ton J. Visser, Philip H. Elsinga, Bauke M. de Jong, Thom W. van der Mark, Jan Kraan, Kees Ensing, Jan Pruim, Antoon T.M. Willemsen, Otto-Erich Brodde, Gerben M. Visser, Anne M.J. Paans and Willem Vaalburg

PET Center, Department of Neurology and Department of Pulmonary Diseases, University Hospital and Department of Analytical Chemistry and Toxicology, University Center for Pharmacy, Groningen, The Netherlands; Institute of Pharmacology and Toxicology, Martin Luther University, Halle/Saale, Germany

We evaluated the suitability of fluorocarazolol for in vivo studies of cerebral beta-adrenoceptors because (*S*)-1′-[^{18}F]fluorocarazolol has a higher affinity to beta-adrenoceptors than to serotonergic receptors (pK_i β_1 9.4, β_2 10.0, 5HT_{1A} 7.4, 5HT_{1B} 8.1) and rapidly crosses the blood-brain barrier. **Methods:** The (*S*)-[^{18}F]fluorocarazolol (74 MBq, >37 TBq/mmol) was intravenously administered to healthy volunteers on two separate occasions with an interval of at least 1 wk. The initial injection was without pretreatment, but before the second injection, the volunteers received the beta blocker (±)-pindolol (3 × 5 mg orally, during 18 hr). The brain was studied with a PET camera in dynamic mode. **Results:** Uptake of radioactivity delineated gray matter and was particularly high in the posterior cingulate, precuneus and striatum. Low uptake occurred in the thalamus, whereas the lowest uptake was observed in the white matter of the corpus callosum. After pindolol pretreatment, uptake was reduced and its distribution became homogeneous throughout the brain. The ratio of total-to-nonspecific binding was about 2 at 60 min, increasing to 2.5–2.75 at longer intervals. **Conclusion:** Fluorocarazolol is the first radioligand that can visualize cerebral beta-adrenoceptors and may enable monitoring of these binding sites during disease.

Key Words: beta-adrenoceptors; brain; PET; fluorine-18-fluorocarazolol

J Nucl Med 1997; 38:934–939

An intriguing problem in biomedical research is that of relating symptoms of neurological as well as psychiatric disturbances to altered neurotransmitter binding in distinct regions of the brain. Cerebral beta-adrenergic binding sites for the neurotransmitter noradrenaline have been reported to be affected in a variety of disorders, such as depression (*1,2*), schizophrenia (*3*), alcoholism (*4*), Alzheimer's disease (*5*) and Huntington's chorea (*6*). They appear to play a role in many physiological and behavioral responses, such as glial proliferation (*7,8*), control of respiration (*9*), processing of visual information (*10*), memory function (*11*) and adaptation to stress (*12*). The generally observed delayed onset of action of antidepressant drugs may occur because downregulation of beta-adrenoceptors and serotonergic receptors takes place only after chronic drug administration (*13,14*). Receptor downregulation could be a prerequisite of the antidepressant activity (*15*). Receptor density may also change when noradrenergic innervation is impaired. Deterioration of noradrenergic neurons occurs such as in the Parkinson dementia complex (*16*).

Most of these observations have been made in autopsy studies, in binding assays to human lymphocytes and cultured cells or in animal experiments. None of these relationships has been observed in intact humans by external detection with receptor-specific radioligands. Fluorocarazolol, a fluorinated analog of the potent beta-blocker carazolol has been useful in in vivo studies of beta-adrenoceptors, both in experimental animals (*17–19*) and in humans (*20*). Uptake in the rat brain is saturable, sensitive to selective beta-adrenoceptor antagonists and stereospecific. We now report the first results obtained with (*S*)-1′-[^{18}F]fluorocarazolol-PET to visualize the distribution of beta-adrenoceptors in the brain of healthy volunteers.

Received May 31, 1996; revision accepted Oct. 23, 1996.

For correspondence or reprints contact: Dr. A. van Waarde, PET Center, Groningen University, Hospital, P.O.Box 30,001, 9700 RB Groningen, The Netherlands.

MATERIALS AND METHODS

Radioligand

(*S*)-Desisopropylcarazolol (enantiomeric excess >98%) was prepared as reported previously (*17*). (*S*)−1′-[^{18}F]fluorocarazolol was synthesized by reacting the precursor with [^{18}F]fluoroacetone (17,19) and purified by HPLC. The specific activity was 75 ± 35 TBq/mmol (2040 ± 950 Ci/mmol) and the radiochemical purity was >99.8%. The ligand was dissolved in 0.5 ml ethanol/propylene glycol/0.9% NaCl (1/2/2 v/v/v). Before injection, this solution was filtered (0.22 μm) and 7.5 ml 0.9% NaCl were added through the filter. The solution was sterile and apyrogenic. (*S*)−1′-fluorocarazolol. HCl passed the test on acute toxicity (European Pharmacopeia; Dutch Pharmacopeia Ed. IX) at a 10,000-fold higher dose than was administered to humans.

In Vitro Binding Assays

The affinity of (*S*)−1′-fluorocarazolol to β_1- and β_2-adrenoceptors was assessed in membranes prepared from human right atrial tissue and human lymphocytes, respectively, using (-)-[^{125}I]iodocyanopindolol as the radioligand (*21*). Affinity of (*S*)−1′-fluorocarazolol to $5HT_{1A}$ receptors was determined in bovine hippocampal membranes using 1.0 n*M* [^{3}H]−8-OH-DPAT as the radioligand; the affinity to $5HT_{1B}$ receptors was measured in rat striatal membranes, using 150 p*M* [^{125}I]iodocyanopindolol in the presence of 60 μ*M* (-)- isoproterenol. The resulting IC_{50} values were converted to K_i values according to the Cheng and Prusoff equation (*22*): $K_i = IC_{50}/([S]/K_d + 1)$, where IC_{50} = concentration of fluorocarazolol that inhibited radioligand binding by 50%, [S] = concentration of radioligand in the assay and K_d = equilibrium dissociation constant of the radioligand. The β_1- and β_2-adrenoceptor assays were performed by the Institut für Pharmakologie und Toxikologie, Halle, Germany; affinities to $5HT_{1A}$ and $5HT_{1B}$ receptors were determined by NovaScreen (Hanover, MD).

Human Volunteers

Healthy volunteers were recruited through advertisements in a local newspaper. Excluded were people with: (a) a positive history regarding neuropsychiatric disease; (b) use of antidepressants, beta-blockers, beta-mimetics or theophylline; (c) high blood pressure or heart failure; or (d) pregnancy or suspected pregnancy. All volunteers had the following screening: medical history, physical examination, routine blood biochemistry to assess kidney and liver function, and electrocardiogram. The study was approved by the Medical Ethics Committee of the Groningen University Hospital. Each subject was informed about the purpose and hazards of the experiment both orally and in writing and gave informed consent.

Study Protocol

At the beginning of the study, a cannula was placed in a vein of one of the lower forearms. Another cannula was placed in a radial artery of the contralateral arm after patency of the ulnar artery had been proven by the Allen test. The arterial cannula was inserted under local anesthesia with lidocain. The venous cannula was used for injection of the ligand, the arterial line for blood sampling.

The volunteer was then placed on the PET camera (Siemens ECAT 951/31, Knoxville, TN, FWHM = 6 mm, axial field of view 10.8 cm, images reconstructed in 31 planes). Volunteers were positioned to the orbito-meatal line. Next, a transmission scan was produced using the internal ^{68}Ge/^{68}Ga sources to correct for attenuation. Cerebral blood flow was assessed by bolus injection of 1.85 GBq (50 mCi) $H_2{}^{15}O$ (using a Medrad OP-100 remote-controlled pump, total volume 40 ml at a speed of 8 ml/sec^{-1}) to make sure that no perfusion defects were present. Data acquisition was started at the onset of injection: four frames of 5 sec were followed by one frame of 10 sec, two frames of 30 sec and one frame of 2 min. Total duration of the study was 3.5 min. After an interval of at least 10 min (i.e., 5 half-lives of ^{15}O), (*S*)−1′-[^{18}F]fluorocarazolol (on average 63 MBq = 1.7 mCi) was injected over a period of 1 min, using the Medrad pump.

Data acquisition was started at the onset of injection: eight frames of 15 sec were followed by four frames of 30 sec, four frames of 1 min, four frames of 2 min, six frames of 4 min and two frames of 10 min. Total duration of the study was 60 min. Arterial blood samples (2 ml) were drawn at 0.5-min intervals during the initial 5 min and at 10-min intervals from 10 to 60 min postinjection. Radioactivity in plasma and in a cell pellet (5 min 3000 g) was determined in all samples using a gamma counter that was cross-calibrated with the PET camera. Additional samples (3 ml) drawn at 1, 2, 5, 10, 20, 40 and 60 min were used for metabolite analysis. Plasma was analyzed for the presence of (*S*)−1′-[^{18}F]fluorocarazolol and radioactive metabolites by direct injection onto an internal-surface reversed-phase column 150 × 4.6 mm; mobile phase 10 m*M* K_2HPO_4:acetonitrile 90:10, pH 7.5; flow rate 1.5 ml.min^{-1}) as published previously (*23*).

After an interval of at least 1 wk, the volunteer returned for the second part of the study in which the influence of a beta-adrenoceptor antagonist on tissue uptake of (*S*)−1′-[^{18}F]fluorocarazolol was assessed. Each volunteer took pindolol orally: 5 mg on the evening before the experiment, 5 mg on the morning before the experiment and 5 mg 60 min before injection of the radioligand.

Cannulas were placed in a vein of each of the lower forearms. No arterial catheter was used in the second part of the study to keep inconvenience to the volunteer to a minimum. One cannula was used for injection and the other for blood sampling. Tracer injection, data acquisition and sampling were performed as on day one.

Data Analysis

ROIs were drawn by hand on white matter (corpus callosum), posterior part of the gyrus cinguli including precuneus, striatum, thalamus and cerebral cortex (comprising both hemispheres in a section just superior to the border of white and gray matter). Time-activity curves for the ROIs were calculated using ECAT software (version 6.5D) running on a Sun/Sparc (Mountain View, CA) workstation. All data were normalized to an injected radioactivity of 74 MBq (2 mCi) and a body weight of 70 kg. The time-activity data were exported to an IBM-compatible PC and characterized using a nonlinear regression data analysis program (EnzFitter, Elsevier Biosoft, Cambridge, U.K.). Differences between groups were tested using one-way analysis of variance and appropriate software (Statistix, NH Analytical, Roseville, MN). A two-tailed probability smaller than 0.05 was considered statistically significant.

RESULTS

General

Preliminary in vitro assays showed that (*S*)−1′-fluorocarazolol binds preferentially to beta-adrenoceptors (pK_i at the β_1-subtype: 9.4, at the β_2-subtype: 10.0) and has less affinity to $5HT_{1A}$ (pK_i 7.4) and $5HT_{1B}$ (pK_i 8.1) serotonergic sites. These results encouraged us to initiate the pilot study in healthy volunteers.

Details regarding the participants and the study protocol are presented in Table 1. None of the volunteers showed any symptoms of heart failure, hypertension or neuropsychiatric disease.

Distribution of Radioactivity within the Brain

The cerebral distribution of the flow tracer, $H_2{}^{15}O$, delineated gray matter as expected. Representative images acquired after injection of *S*-1′-[^{18}F]fluorocarazolol are presented in Figure 1. Transaxial cross-sections in the time frame 14−60 min are

TABLE 1
Volunteers and Study Protocol

Date	Volunteer no.	Age (yr)	Sex	Weight (kg)	Pre-treatment	Injected mass (nmol)	Scan type
05-24-95	1	36	M	67	None	0.88	Static
05-31-95	1				Pindolol	1.01	Static
07-12-95	2	55	M	82	None	0.68	Dynamic
07-19-95	2				Pindolol	0.67	Dynamic
08-02-95	3	27	F	56	None	1.75	Static
09-20-95	3				Pindolol	0.59	Static
11-01-95	4	21	M	72	None	0.40	Dynamic
11-08-95	4				Pindolol	0.35	Dynamic
11-29-95	5	28	M	76	None	1.33	Static
12-13-95	6	22	F	70	None	1.57	Dynamic
01-03-96	6				Pindolol	0.67	Dynamic
01-17-96	7	21	M	69	None	0.24	Dynamic
02-28-96	7				Pindolol	0.71	Dynamic
02-14-96	8	25	M	70	None	0.27	Dynamic
Mean ± s.d.		29 ± 11 (8)		70 ± 7 (8)		0.79 ± 0.47 (14)	

displayed. In the initial study (without pindolol), gray matter was clearly demarcated from white matter. Uptake of radioactivity was especially high in the cortical areas (posterior cingulate, precuneus) and the corpus striatum (caudate and putamen, Fig. 1). Low uptake occurred in the thalamus. The lowest uptake was observed in the white matter (corpus callosum, see Fig. 1). This relatively high striatal uptake and low uptake in the thalamus contrasted with the more even distribution of radioactivity seen in the $H_2{}^{15}O$ scans. In one volunteer, a hot spot was visible just ventrally to the cerebellum and interpreted as the putative locus coeruleus (see Fig. 1). After ingestion of pindolol, cerebral uptake of radioactivity was strongly (>two-fold) suppressed and gray matter was no longer demarcated, as the distribution of radioactivity became virtually homogeneous throughout the brain (see Fig. 1 and Table 2). The hot spot near the cerebellum also disappeared after preloading of the volunteer with pindolol.

Kinetics of Cerebral (S)−1′-[^{18}F]Fluorocarazolol Uptake

After injection of the radioligand, cortical levels of radioactivity rapidly rose to a maximum followed by an equally rapid, small decline to a relatively stable plateau that was reached within 3 min (Fig. 2). Pindolol accelerated the washout of radioactivity from the cortex (Fig. 2) and it reduced cortical radioactivity to <50% of the control at 60 min postinjection. In contrast to the data for cerebral cortex, uptake of radioactivity in the white matter of the corpus callosum was not significantly affected by pindolol (Fig. 2). Uptake in the corpus callosum was about equal to that in the cortex of pindolol-treated subjects at >30 min postinjection (Fig. 2).

If uptake of radioactivity in the presence of pindolol is considered to represent nonspecific binding, ratios of total-to-nonspecific binding can be calculated. In the cerebral cortex, this parameter increased during the whole period of PET scanning, and it was not yet maximal after 60 min (Fig. 3). The curve fitted to the data suggests that a maximum of 2.52 is reached with a first-order rate constant of 0.0222 min^{-1} (i.e., time required to reach 50% of the maximum = 31 min).

Washout of radioactivity from the brain of untreated subjects is slow and it appears to be different in different brain areas (faster in thalamus than in other areas of the brain). The relative amount of radioactivity which remains in different areas at 60

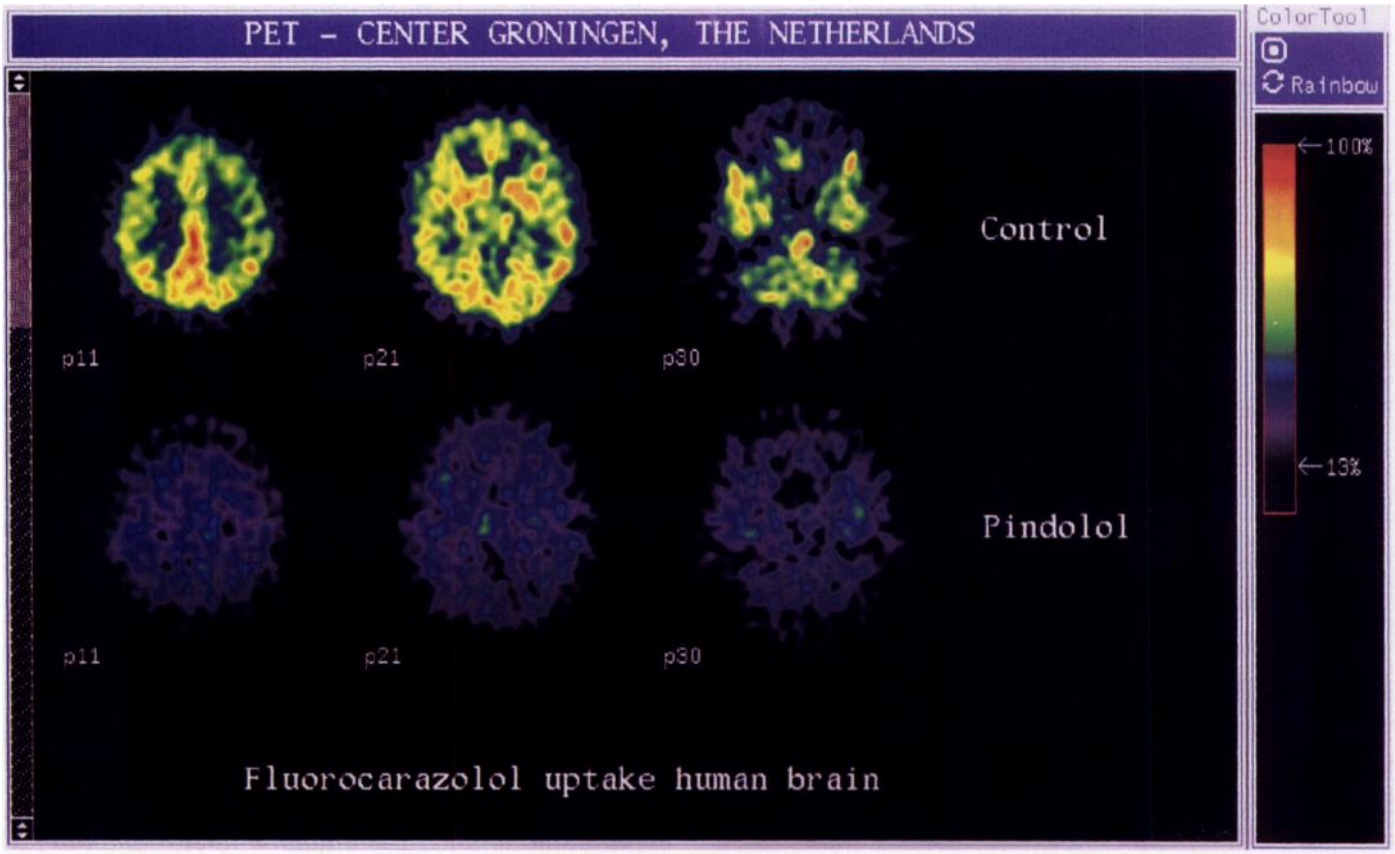

FIGURE 1. PET brain images at the level of the cingulate cortex + precuneus, striatum and locus coeruleus (from left to right). The upper row of images was acquired in the untreated condition; the lower row after the volunteer had ingested pindolol (time frame 14–60 min). The volunteer is on his back; the direction of observation is from his feet towards his head.

TABLE 2
Uptake of Fluorine-18 in Different Brain Areas 20–60 min Postinjection

Area	Untreated	Pindolol-preloaded
Cingulate	14.6 ± 0.8	6.2 ± 0.5*
Striatum	14.3 ± 0.8	6.3 ± 0.6*
Superficial layers of the cortex	12.9 ± 0.9	6.9 ± 0.9*
Thalamus	8.3 ± 0.9	5.6 ± 0.3*
White matter	6.3 ± 0.4	5.7 ± 0.9

*Significant differences between the untreated and pindolol-preloaded condition (one-way ANOVA $P < 0.05$).

Tissue uptake of radioactivity is expressed as camera units (ECAT cts/pixel/sec) × 10^4. Data are an average ± s.e.m. of all dynamic studies (five in the control condition, four after pindolol preload); values were normalized to an injected dose of 74 MBq (2 mCi).

min is: cingulate cortex plus precuneus = striatum > other parts of the cortex > thalamus > white matter of the corpus callosum.

Effect of Beta-Blockade on Radioligand Clearance and Metabolism

Preloading of volunteers with pindolol affects clearance and metabolism of the radioligand (Fig. 4). Levels of radioactivity in the circulation at 20–60 min postinjection are higher, and the fraction of plasma radioactivity representing parent compound also is higher after treatment of volunteers with pindolol. Similar results had been obtained in a previous study of beta-adrenoceptors in the human thorax (*20*).

DISCUSSION

Selectivity of Fluorocarazolol

Many beta-blockers interact with central serotonergic sites (*24–26*). Iodocyanopindolol (*24,26*), pindolol (*27*), carteolol (*25*) and propranolol (*25,27*) bind almost equally well to $5HT_{1A}$ and/or $5HT_{1B}$ receptors as to beta-adrenoceptors. In contrast, hydrophilic atenolol (*25*) and CGP-12177 (*26*) are selective beta-adrenoceptor antagonists. Unfortunately, ^{11}C-atenolol and ^{11}C-CGP 12177 cannot be used for PET studies of the brain as CGP 12177 hardly crosses the blood-brain barrier (*28,29*), while the affinity of atenolol is too low for succesful beta-adrenoceptor imaging (*30*). Because of its lipophilicity [log P 2.2 at pH 7.4, (*19*)], fluorocarazolol was expected to show rapid transport over the blood-brain barrier. Indeed, we have observed that (*S*)-1′-[^{18}F]fluorocarazolol enters rat brain and it demonstrates significant specific binding in cerebral cortex and cerebellum (*18*). In vitro binding assays have shown a much higher affinity of fluorocarazolol to beta-adrenoceptors than to $5HT_{1A}$ or $5HT_{1B}$ receptors (see Results). The 20- to 400-fold selectivity of fluorocarazolol for beta-adrenoceptors indicates that serotonergic sites will not significantly contribute to the specific binding in the brain after administration of a nanomolar dose of the radioligand (see also below).

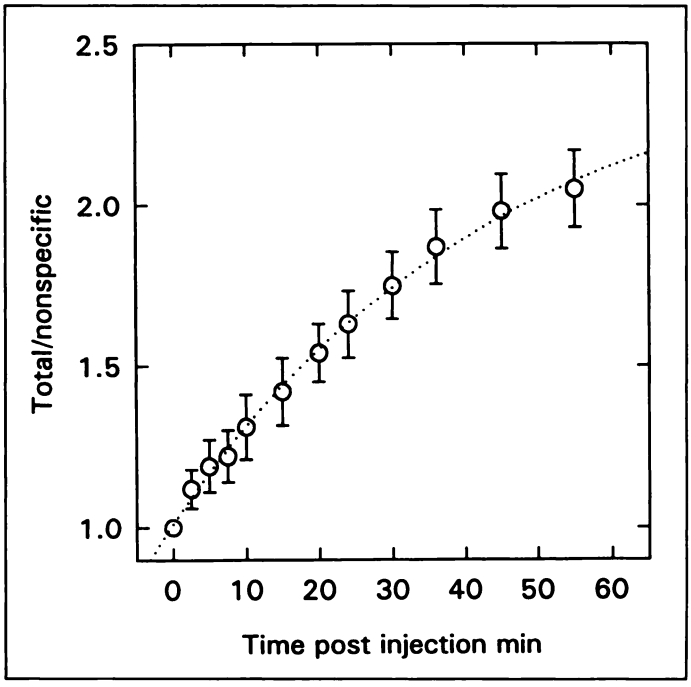

FIGURE 3. Ratios of total/nonspecific binding in cerebral cortex, calculated from tissue uptake of (*S*)-1′-[^{18}F]fluorocarazolol in the presence and absence of pindolol (mean ± s.e. of four volunteers).

Distribution of Binding Sites for Fluorocarazolol within the Brain

Whether a ligand binds to receptors in the living human brain can be determined by assessing whether the regional distribution of radioactivity after drug injection parallels the distribution of receptors known from post mortem autoradiography, and by examining whether administration of an excess of an

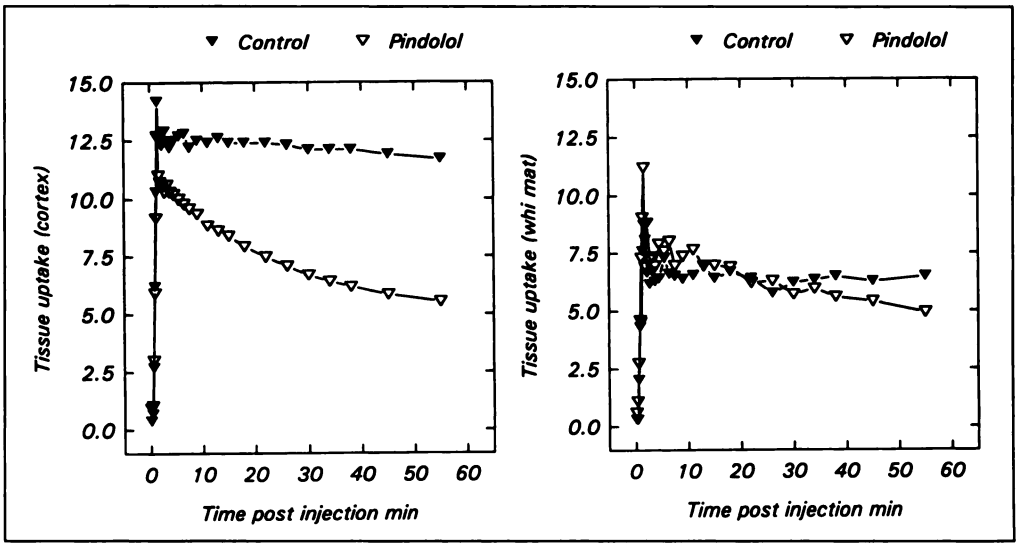

FIGURE 2. Time-activity curves in two areas of the human brain after injection of (*S*)−1′-[^{18}F]fluorocarazolol. Data are an average of all dynamic studies (five in the untreated condition, four after ingestion of pindolol; values were normalized to an injected dose of 74 MBq [2 mCi]). Tissue uptake of radioactivity is expressed as camera units (ECAT cts/pixel/sec) × 10^4.

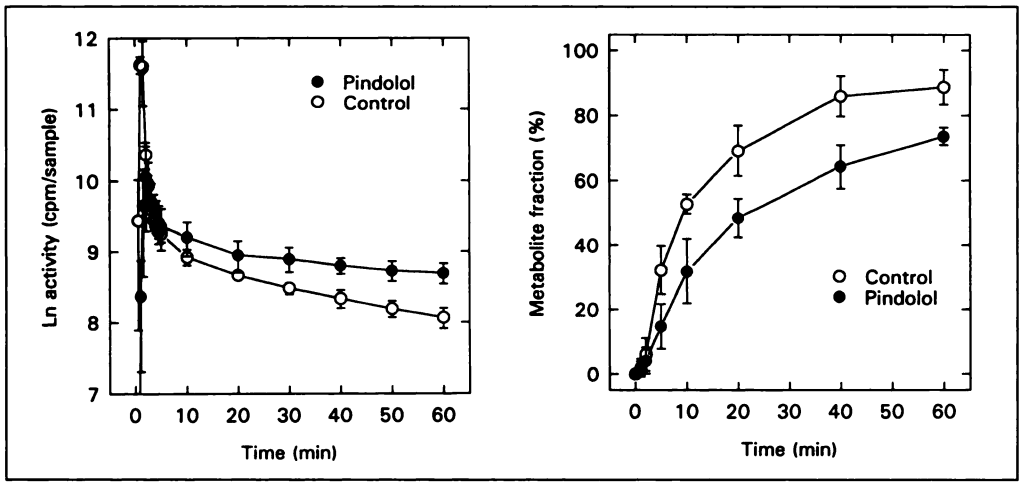

FIGURE 4. Clearance of ^{18}F from human plasma after injection of (*S*)-1′-[^{18}F]fluorocarazolol, and the fraction of plasma radioactivity representing metabolites. Data are an average of all dynamic studies (five in the untreated condition, four after ingestion of pindolol; values were normalized to an injected dose of 74 MBq [2 mCi]).

unlabeled receptor antagonist blocks this specific regional distribution. Both approaches were used in this study.

After administration of (*S*)-1′-[^{18}F]fluorocarazolol to volunteers, distribution of radioactivity within the brain was inhomogeneous. Relatively high uptake was observed in the striatum and cortical areas (especially cingulate cortex and precuneus). Low levels of radioactivity were present in the thalamus and the lowest in white matter. Such a distribution corresponds to the localization of β-adrenoceptors known from post mortem autoradiography with the ligands [^{125}I]iodocyanopindolol, [^{125}I]iodopindolol and [^{3}H]CGP 12177: high beta-adrenoceptor densities are found in caudate and putamen (*2,13,31–33*), moderate to high densities in various cortical areas (*2,13,31–33*) and low densities in thalamus (*2,13,32*) and white matter (*33,34*). With the most selective beta-adrenoceptor ligand, [^{3}H]CGP-12177, the following receptor densities were measured: caudate/putamen 100–134, cortex 55–80, thalamus 38–45 and white matter <20 fmol/mg protein (*1,2,13,31*). If we assume that 10% of tissue wet weight consists of protein, receptor densities in cortex range from 5.5–8.0 pmol/g. The cerebral concentration of fluorocarazolol in this study was < 0.03 pmol/ml. Thus, beta-adrenoceptor occupancy by fluorocarazolol was negligible (i.e., <0.5%).

In one volunteer (Volunteer 2), the putative locus coeruleus was delineated after injection of (*S*)−1′-[^{18}F]fluorocarazolol. The locus coeruleus does not contain a particularly high amount of beta-adrenoceptors, but strong nonspecific binding of [^{125}I]iodocyanopindolol has been reported in this region, which is probably related to the presence of neuromelanin (*32*). The observation that a pindolol preload suppresses uptake of ^{18}F in the pons of Volunteer 2 (Fig. 1) suggests that binding of fluorocarazolol, in contrast to that of iodocyanopindolol, is not truly nonspecific but takes place to non-beta-adrenergic sites as has been reported for iodocyanopindolol in the heart (*35*).

Blockage of the Specific Regional Distribution by an Unlabeled Beta-Adrenoceptor Antagonist

Pindolol is a nonsubtype-selective beta-adrenoceptor antagonist with substantial affinity to $5HT_{1A}$ receptors (*27*). Other beta-blockers that penetrate the brain and are registered as drugs, such as propranolol, bind even to $5HT_{1A}$- and $5HT_{1B}$-sites (*25*). We selected pindolol for our blocking experiments because the drug has intrinsic sympathomimetic activity; undesired side effects on heart rate and sleep are less frequent after ingestion of pindolol than of propranolol.

Pindolol induced a more rapid washout of (*S*)-1′-[^{18}F]fluorocarazolol-derived radioactivity from receptor-containing areas of the brain but not from areas with very low receptor density such as the white matter of the corpus callosum (Fig. 2). Local differences in tissue uptake of radioactivity within the brain observed 14–60 min after injection of the radioligand were absent when the volunteers had ingested pindolol (Fig. 1). Uptake in all regions then became similar to that in the corpus callosum. Thus, administration of an excess of an unlabeled receptor antagonist blocked the specific regional distribution of (*S*)-1′-[^{18}F]fluorocarazolol within the brain.

CONCLUSION

(*S*)-1′-[^{18}F]fluorocarazolol, a potent beta-adrenergic receptor antagonist, specifically accumulated in gray matter after in vivo administration to humans. Uptake is particularly high in the striatum and in various cortical areas, regions with a high density of beta-adrenoceptors. Preferential localization in striatum and cortex is blocked by administration of an excess of an unlabeled beta-adrenoceptor antagonist (pindolol). These data, combined with results from animal experiments, indicate that the distribution of radioactivity reflects radioligand binding to beta-adrenoceptors. White matter of the corpus callosum can probably be used as a reference region to estimate nonspecific binding. It may now be feasible to assess the role of human cerebral beta-adrenoceptors in the action of antidepressant drugs and in disorders such as depression and schizophrenia.

ACKNOWLEDGMENTS

This project was supported by Netherlands Asthma Foundation grant AF 92.20.

REFERENCES

1. De Pärmentier F, Cheetham SC, Crompton MR, Katona CL, Horton RW. Brain beta-adrenoceptor binding sites in antidepressant-free depressed suicide victims. *Brain Res* 1990;525:71–77.
2. De Pärmentier F, Crompton MR, Katona CL, Horton RW. Beta-adrenoceptors in brain and pineal from depressed suicide victims. *Pharmacol Toxicol* 1992;711(suppl):86–95.
3. Joyce JN, Lexow N, Kim SJ, et al. Distribution of beta-adrenergic receptor subtypes in human post-mortem brain: alterations in limbic regions of schizophrenics. *Synapse* 1992;10:228–246.
4. Valverius P, Borg S, Valverius MR, Hoffman PL, Tabakoff B. Beta-adrenergic receptor binding in brain of alcoholics. *Exp Neurol* 1989;105:280–286.
5. Kalaria RN, Andorn AC, Tabaton M, Whitehouse PJ, Harik SI, Unnerstall JR. Adrenergic receptors in aging and Alzheimer's disease: increased β_2-receptors in prefrontal cortex and hippocampus. *J Neurochem* 1989;53:1772–1781.
6. Wëber C, Rigo M, Chinaglia G, Probst A, Palacios JM. Beta-adrenergic receptor subtypes in the basal ganglia of patients with Huntington's chorea and Parkinson's disease. *Synapse* 1991;8:270–280.
7. Sutin J, Griffith R. Beta-adrenergic receptor blockade suppresses glial scar formation. *Exp Neurol* 1993;120:214–222.
8. Hodges-Savola C, Rogers SD, Ghilardi JR, Timm DR, Mantyh PW. Beta-adrenergic receptors regulate astrogliosis and cell proliferation in the central nervous system in vivo. *Glia* 1996;17:52–62.
9. Annane D. Médiation beta-adrenergique de la commande centrale de la ventilation: mythe ou realité? *J Toxicol Clin Exp* 1991;11:325–336.

10. Maloteaux JM. Drug and transmitter receptors in human brain. Characterization and localization of serotonin, dopamine and adrenergic receptors. *Acta Neurol Belg* 1986;86:61–129.
11. Flexner JB, Flexner LB, Church AC, Rainbow TC, Brunswick DJ. Blockade of beta-1 but not of beta-2 adrenergic receptors replicates propranolol's suppression of the cerebral spread of an engram in mice. *Proc Natl Acad Sci USA* 1985;82:7458–7461.
12. Stone EA, Platt JE. Brain adrenergic receptors and resistance to stress. *Brain Res* 1982;237:405–414.
13. De Paermentier F, Cheetham SC, Crompton MR, Katona CL, Horton RW. Brain beta-adrenoceptor binding sites in depressed suicide victims: effects of antidepressant treatment. *Psychopharmacology* 1991;105:283–288.
14. Garattini S, Samanin R. Drugs: guide and caveats to explanatory and descriptive approaches–I. A critical evaluation of the current status of antidepressant drugs. *J Psychiatr Res* 1984;18:373–390.
15. Okada F, Tokumitsu Y. Is the β-downregulation a prerequisite of the antidepressant activity? *J Psychopharmacol* 1994;8:62–63.
16. Jellingen KA. Pathology of Parkinson's disease: changes other than the nigrostriatal pathway. *Mol Chem Neuropathol* 1991;14:153–197.
17. Elsinga PH, Vos MG, Van Waarde A, et al. (*S,S*)- and (*S,R*)-1′-[^{18}F]flu-orocarazolol, ligands for the visualization of pulmonary β-adrenergic receptors with PET. *Nucl Med Biol* 1996;23:159–167.
18. Van Waarde A, Elsinga PH, Brodde OE, Visser GM, Vaalburg W. Myocardial and pulmonary uptake of (*S*)-1′-[^{18}F]fluorocarazolol in intact rats reflects radioligand binding to β-adrenoceptors. *Eur J Pharmacol* 1995;272:159–168.
19. Zheng LB, Berridge MS, Ernsberger P. Synthesis, binding properties, and ^{18}F labeling of fluorocarazolol, a high-affinity β-adrenergic receptor antagonist. *J Med Chem* 1994;37:3219–3230.
20. Visser TJ, Van Waarde A, van der Mark TW, et al. Characterization of thoracic β-adrenoceptors in healthy volunteers using fluorocarazolol-PET [Abstract]. *J Nucl Med* 1996;37(suppl):71P.
21. Brown L, Deighton NM, Bals S, Spare receptors for beta-adrenoceptor-mediated positive inotropic effects of catecholamines in the human heart. *J Cardiovasc Pharmacol* 1992;19:222–232.
22. Cheng YC, Prusoff WH. Relationship between the inhibition constant (K_i) and the concentration of inhibitor which causes 50 per cent inhibition (IC_{50}) of an enzymatic reaction. *Biochem Pharmacol* 1973;22:3099–3108.
23. Van Waarde A, Visser TJ, Posthumus H, et al. Quantification of the β-adrenoceptor ligand, (*S*)-1′-[^{18}F]-fluorocarazolol, in plasma of humans, rats and sheep. *J Chromatogr B* 1996;678:253–260.
24. Edwards E, Whitaker-Azmitia PM. Selective beta-antagonists are equally and highly potent at 5-HT sites in the rat hippocampus. *Neuropharmacology* 1987;26:93–96.
25. Nishio H, Nagakura Y, Segawa T. Interactions of carteolol and other beta-adrenoceptor blocking agents with serotonin receptor subtypes. *Arch Int Pharmacodyn Ther* 1989;302:96–106.
26. Morin D, Zini R, Urien S, Sapena R, Tillement JP. Labeling of rat brain beta-adrenoceptors: (^{3}H)CGP-12177 or (^{125}I)iodocyanopindolol? *J Recept Res* 1992;12: 369–387.
27. Oksenberg D, Peroutka SJ. Antagonism of 5-hydroxytryptamine$_{1A}$ (5-HT$_{1A}$) receptor-mediated modulation of adenylate cyclase activity by pindolol and propranolol isomers. *Biochem Pharmacol* 1988;37:3429–3433.
28. Van Waarde A, Meeder JG, Blanksma PK, et al. Suitability of CGP12177 and CGP26505 for quantitative imaging of β-adrenoceptors. *Nucl Med Biol* 1992;19:711–718.
29. Van Waarde A, Meeder JG, Blanksma PK, et al. Uptake of radioligands by rat heart and lung in vivo: CGP12177 does and CGP26505 does not reflect binding to β-adrenoceptors. *Eur J Pharmacol* 1992;222:107–112.
30. Van Waarde A, Elsinga PH, Anthonio RL, et al. Study of cardiac receptor ligands by positron emission tomography. In: Van der Wall EE, Blanksma PK, Niemeyer MG, et al, eds. *Cardiac positron emission tomography: viability, perfusion, receptors and cardiomyopathy.* Dordrecht, Germany: Kluwer Academic Publishers;1995:171–182.
31. De Pärmentier F, Cheetham SC, Crompton MR, Horton RW. Beta-adrenoceptors in human brain labeled with [^{3}H]dihydroalprenolol and [^{3}H]CGP 12177. *Eur J Pharmacol* 1989;167:397–405.
32. Pazos A, Probst A, Palacios JM. Beta-adrenoceptor subtypes in the human brain: autoradiographic localization. *Brain Res* 1985;358:324–328.
33. Reznikoff GA, Manaker S, Rhodes CH, Winokur A, Rainbow TC. Localization and quantification of beta-adrenergic receptors in human brain. *Neurology* 1986;36:1067–1073.
34. Arango V, Ernsberger P, Marzuk PM, et al. Autoradiographic demonstration of increased serotonin 5-HT$_2$ and beta-adrenergic receptor binding sites in the brain of suicide victims. *Arch Gen Psych* 1990;47:1038–1047.
35. Bjornerheim R, Golf S, Hansson V. Specific non-beta-adrenergic binding sites for [^{125}]I-iodocyanopindolol in myocardial membrane preparations: a comparative study between human, rat and porcine hearts. *Cardiovasc Res* 1991;25:764–773.

Cerebral Sparganosis: Increased Uptake of Technetium-99m-HMPAO

Dong-Ling You, Kai-Yuan Tzen, Pan-Fu Kao, Yat-Sen Ho and Chun-Che Chu
Departments of Nuclear Medicine, Pathology and Neurology, Chang Gung Memorial Hospital, Taipei, Taiwan

Cerebral sparganosis is an extremely rare intracranial parasitic infectious disease. We report findings of ^{99m}Tc-HMPAO cerebral perfusion SPECT in a case with cerebral sparganosis. SPECT revealed an irregularly shaped area with markedly increased ^{99m}Tc-HMPAO uptake in the parasitic infectious region of the cerebrum. Both white and gray matter was involved, the white matter involved predominantly. Decreased perfusion to the right cerebellum, suggesting cross cerebellar diaschisis, was also demonstrated. This article illustrates that cerebral sparganosis is one of the causes of increased ^{99m}Tc-HMPAO uptake in the cerebrum and should be considered clinically if present.

Key Words: sparganosis; technetium-99m-HMPAO; cerebral perfusion SPECT

J Nucl Med 1997; 38:939–941

Cerebral sparganosis is an extremely rare central nervous system (CNS) parasitic infectious disease caused by the plerocercoid larva, called sparganum, of Spirometra mansonoides (*1,2*). Most cases of cerebral sparganosis have been reported from Korea, Japan, China, Taiwan and Southeast Asia (*2–9*). This article demonstrates the findings of ^{99m}Tc-HMPAO cerebral perfusion SPECT in a case with cerebral sparganosis.

CASE REPORT

A 74-yr-old man patient presented to our hospital with seizure and progressive weakness of the right side of his body for 1 mo. The patient did not have a fever. Neurological examination revealed decreased sensation and muscle power of the right side of the body. The white blood cell count on admission was 5,900/mm^3, and the differentiation showed 70% granulocytes, 19% lymphocytes, 4% eosinophils and 7% monocytes. EEG revealed continuous, focal, slow waves over the left frontotemporoparietal area. Brain CT revealed a cystic, enhancing mass lesion at left temporal area (Fig. 1). Brain MRI also revealed a mass lesion with hypointensity on T1-weighted images and hyperintensity on T2-weighted images (Fig. 1) with heterogeneous enhancement at the left temporal area. Based on the clinical presentations, examinations, CT and MRI findings brain tumor was suspected.

Technetium-99m-HMPAO cerebral perfusion SPECT was arranged to evaluate the regional blood flow to the intracranial mass lesion. SPECT imaging was performed using a triple-head gamma camera equipped with fan-beam collimators. Acquisition was started 20 min after an intravenous injection of 925 MBq (25 mCi) ^{99m}Tc-HMPAO in 120 projections, 3° apart, in a 128 × 128 matrix.

Received Jun. 12, 1996; accepted Oct. 15, 1996.
For correspondence or reprints contact: Dong-Ling You, MD, Department of Nuclear Medicine, Chang Gung Memorial Hospital, 199 Tung-Hwa North Rd., Taipei, Taiwan, R.O.C.